J Mol Model (2010) 16:749–757
DOI 10.1007/s00894-009-0593-z

ORIGINAL PAPER

Computational (DFT and TD DFT) study of the electron structure of the tautomers/conformers of uridine and deoxyuridine and the processes of intramolecular proton transfers

Vassil B. Delchev

Received: 14 July 2009 / Accepted: 14 September 2009 / Published online: 10 October 2009
© Springer-Verlag 2009

Abstract Six uridine and six deoxyuridine isomers were studied at the B3LYP and TD B3LYP theoretical level and 6–31+G(d) basis function. The stability and the excited states of the isomers were studied in order to clarify some known experimental data. It was established that the rotation of the oxo uracil ring in uridine is energetically more likely to occur in the excited state than in the ground state, driven by the bright $^1\pi\pi^*$ state and the dark charge transfer $^1n\pi^*$ state. Very high energy barriers (on the S_o) were found for thermal intramolecular proton transfer processes.

Keywords Deoxyuridine · DFT calculation · Excited state · Excitation energy · Proton transfer · Uridine

Introduction

Uridine and deoxyuridine are RNA nucleosides that play a crucial biological role in the living world and medicine. For many years, nucleoside analogues (called nukes) have been the cornerstone of combinatory therapy to treat HIV/AIDS [1]; examples include zidovudine (Retrovir), astavudine (Zerit), etc. Many of these drugs, give rise to nucleosides during decomposition in the body. For example, the drug triacetyluridine (TAU) is converted to uridine in the body. TAU has been tested in HIV-negative people with cancers as well as in others with degenerative diseases of the nervous system, such as Alzheimer's and Parkinson's diseases. Some tests have been carried out with TAU for the treatment of conditions such as major depression [1].

Uridine has beneficial effects in mitochondrial toxicity [2, 3] and antidepressant-like effects [4]. It is a possible endogenous antiepileptic modulator, with anticonvulsant effects in some models of epilepsy. It could be that the H-bonding of uridine with some receptors in the body is responsible for the large selectivity of this nucleoside in some cases. For example, uridine selectivity of three phospholipase C-activating P2 receptors has been studied [5].

Some nonlinear optical rotations have been calculated with density functional theory (DFT) methodology for two conformations of uridine [6]. However, the present study was carried out with the main goal of interpreting experimental results on nonlinear optical rotation of a limited number of uridine conformers (two); the mechanism of proton transfer is not discussed here.

Bureekaew et al. [7] reported (from SAC-CI calculations) that the first excited state in uridine is the bright $^1\pi\pi^*$ state. However, uracil is known to be the primary chromophore in uridine and deoxyuridine and this should determine the ordering of the first few excited states in uridine and deoxyuridine. Describing the excited states of uracil has been the object of many theoretical and experimental studies [8–11]. All have reported that the first excited state of uracil is the dark $^1n\pi^*$ state. The bright $^1\pi\pi^*$ state of uracil is the second excited state. There is no information about the ordering of the excited states of uridine and deoxyuridine studied by time-dependent (TD) DFT methods.

Neutral and protonated conformations of several uridine derivatives have been studied with respect to the ring conformation of furanose and the orientation of the base in relation to ribose [12]. The results have shown the large

V. B. Delchev (✉)
Department of Physical Chemistry, University of Plovdiv,
Tzar Assen Str. 24,
4000 Plovdiv, Bulgaria
e-mail: vdelchev@uni-plovdiv.bg

influence of the sugar substituent on the conformation of the neutral form of these nucleosides.

The crystal structures of uridine and deoxyuridine were elucidated long ago by Green et al. [13] and Rahman et al. [14], respectively. It was shown that the oxo form of uridine and deoxyuridine dominate in the crystal state. A space group of $P2_1$ has been found for both compounds.

Conformations of 2-deoxyuridine have been investigated using Fourier transform infrared (FTIR) matrix isolation spectroscopy and ab initio calculations at HF/3–21G (p), HF/6–31G (d,p) and MP2/6–31G (d,p) levels [15]. The stabilising role of H-bonds in these compounds has been discussed. Nevertheless, there is a gap in our knowledge of the tautomers of uridine and deoxyuridine with respect to the orientation of the uracil moiety. The mechanisms of the tautomeric conversions are also not known.

The purpose of the current study is to shed light on the stability of the tautomers/conformers of uridine and deoxyuridine, and the mechanisms of intermolecular proton transfer. A challenging task in this research is to test the accuracy of the TD DFT method in prediction of the position of the excited states of isomers. The study also includes calculation of the electronic and geometrical structures of the transition states between pairs of tautomeric forms.

The uracil tautomers involved in nucleosides are shown in Scheme 1.

There is one additional uracil tautomer (not given in Scheme 1) that is obtained from oxo uracil by proton transfer between the O atom at the C_2 position and the H atom at the N_1 position. This tautomer cannot be obtained in nucleosides since the N_1 position of uracil is blocked by the sugar residue.

Computational methods

The ground state equilibrium geometries of furanoses and nucleosides were optimised at the B3LYP/6–31+G(d) theoretical level. Subsequent frequency calculations were carried out to prove that the compounds correspond to real minima and to find their thermodynamic functions. The thermodynamic functions of the condensation reactions (deoxy)ribose + uracil → nucleoside + water were found (at 298 K, in the gas phase) according to the equations [16]:

$$\Delta H^o = H_f^o\{nucleoside\} + H_f^o\{water\} - H_f^o\{(deoxy)ribose\} - H_f^o\{uracil\} \quad (1)$$

$$\Delta G^o = G_f^o\{nucleoside\} + G_f^o\{water\} - G_f^o\{(deoxy)ribose\} - G_f^o\{uracil\} \quad (2)$$

$$\Delta S^o = (\Delta H^o - \Delta G^o)/298 \quad (3)$$

The vertical excitation energies of the compounds–minima were found at the TD B3LYP level with the same basis set. The use of diffuse functions in the basis set makes possible to find the repulsive $^1\pi\sigma^*$ state among the four low-lying excited states.

The conformational transformations (with respect to the uracil and sugar rings) of oxo nucleosides (most stable) were studied at the TD DFT level. The starting point in each case was the optimised geometry of the most stable oxo (deoxy) uridine isomer. The next step was the generation of structures/conformers by changing the dihedral angles which are responsible for the rotation of the two rings to one another. More than 20 conformers of (deoxy)uridine were generated in this way. Three singlet excited states were calculated for each conformer, which corresponds vertically to the points on the ground state curve.

The transition states of the intramolecular proton transfer processes were found with the help of the QST2 procedure included in the GAUSSIAN 98 program package [17]. The procedure requires two optimised structures as input: the structure of the initial compound (reactant) and the structure of the final compound (product).

All calculations were carried out with the GAUSSIAN 98 program package [17]. Visualisation of the optimised geometries was performed with the program ChemCraft 1.5 (Build 282) [18].

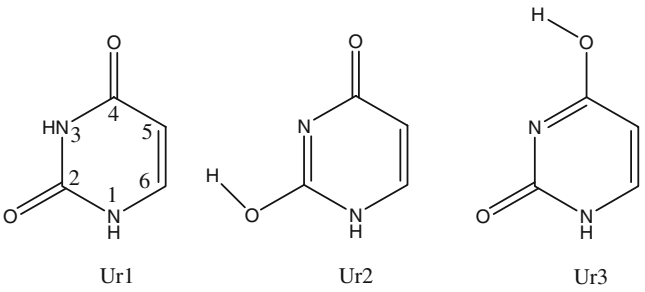

Scheme 1 Uracil tautomers involved in nucleosides (numbering in Ur1 is according to IUPAC)

Results and discussion

Geometries of the tautomers/conformers

The starting point of the current research was the optimisation of the structures of ribose and deoxyribose. Their nucleosides with uracil, i.e. uridine and deoxyuridine, were also optimised at the B3LYP/6–31+G(d) level of theory. All structures are illustrated in Fig. 1.

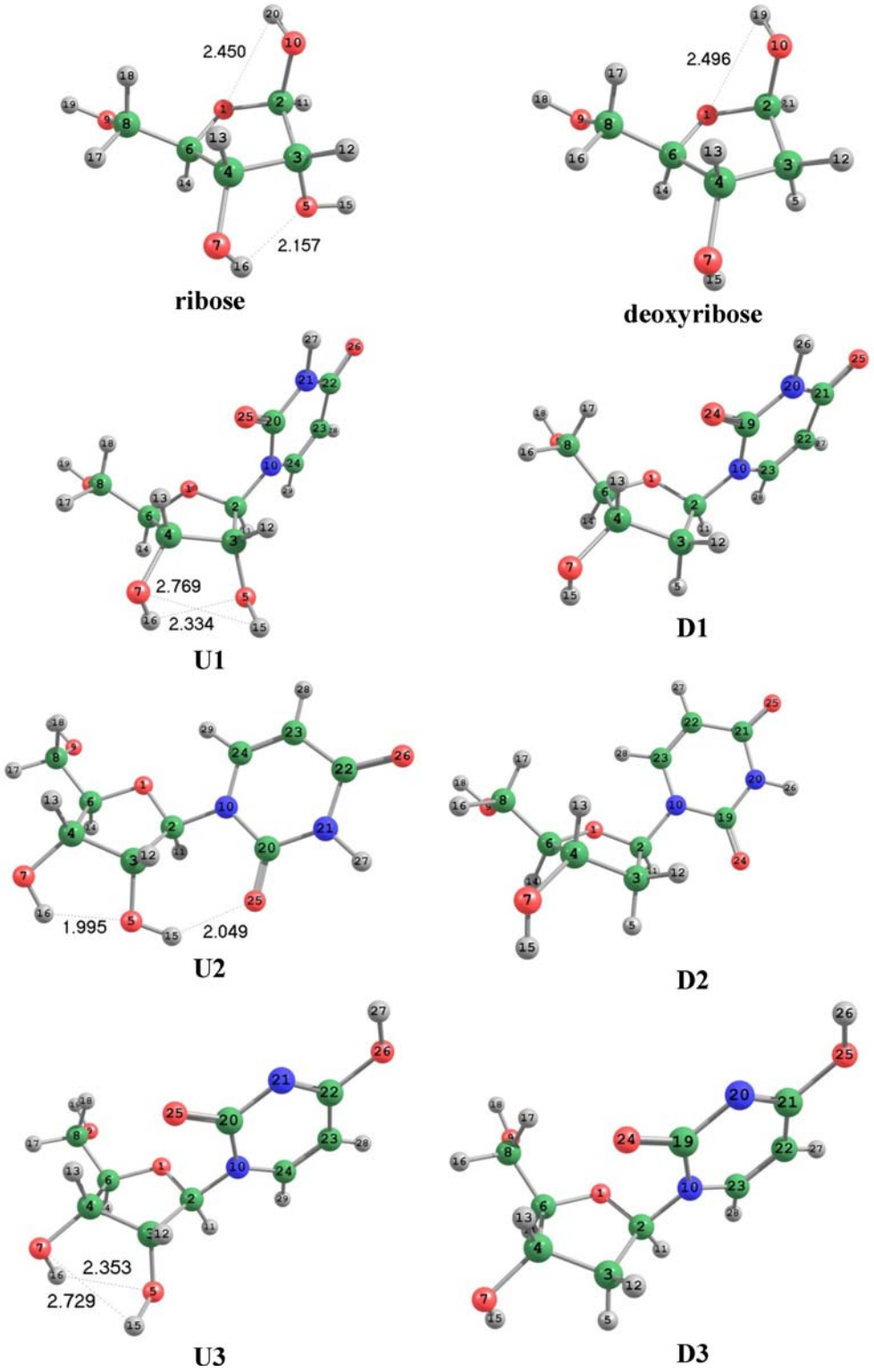

Fig. 1 Optimised structures of the furanoses and nucleosides. *Green* Carbon atoms, *red* oxygen atoms, *blue* nitrogen atoms, *grey* hydrogen atoms

The most stable conformations of all compounds with respect to the sugar ring were initially found by using the molecular mechanics force field. Because of the large size of the investigated molecules we restricted the basis set to one polarisation function and diffuse sp-functions to heavy atoms.

As seen in Fig. 1, the compounds U1/U2, U3/U4, U5/U6 as well as D1/D2, D3/D4, D5/D6 are conformers with respect to the positions of the two rings. However, the compounds U1/U3/U5, and U2/U4/U6 as well as D1/D3/D5, and D2/D4/D6 are functional isomers. The isomers U1/U3/U5 and U2/U4/U6 have different orientations of

Fig. 1 (continued)

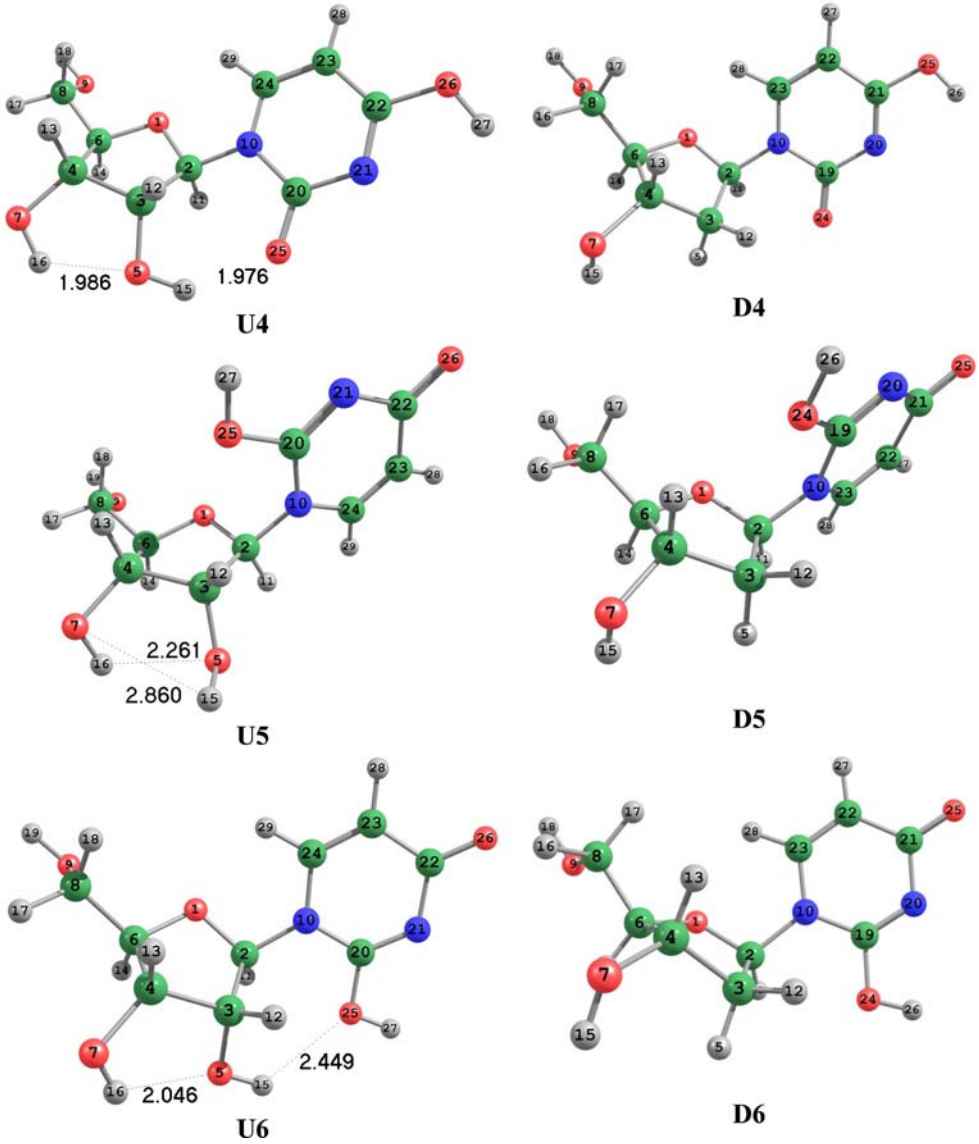

the uracil residue towards the sugar ring. In the first group of functional isomers (U1/U3/U5), the oxygens of uracil are orientated in the vicinity of the furanose ring, whereas in the second group (U2/U4/U6) they are orientated to the opposite side. This is also valid for deoxyuridine isomers.

The structures in Fig. 1 show that at least two H-bonds are formed in all uridine isomers because of the presence of one OH group at the C_3 position (of furanose). Such bonds cannot be observed in deoxyuridines. The calculations showed that the shortest H-bonds are formed between the closest OH groups of the sugar ring, in particular the H-bonds $H_{16}\cdots O_5$. When the oxygen atom O_{25} forms H-bonds with the closest sugar OH group (e.g. $O_{25}\cdots H_{15}$) then the bonds $H_{16}\cdots O_5$ become extremely short.

Stability of the isomeric forms

The calculated energies and relative energies of the ribose and deoxyribose nucleosides are given in Table 1.

As seen from the data in Table 1, the most stable nucleosides are U2 and D2. This result is in full agreement with the crystal structures of the two compounds [13, 14]. The next nucleosides exhibiting considerable stability are U1 and D1. They also contain the oxo form of uracil. High energies were calculated for isomers containing the uracil tautomer with a semiquinonic structure.

As expected, all condensation reactions are thermodynamically and enthalpically disfavoured (Table 1) in the gas phase. One exception is the condensation reaction leading to the production of the nucleoside U4. A possible reason for this is the formation of short H-bonds between the furanose

Table 1 Energies of nucleosides and thermodynamic functions (at 298 K, in the gas phase) of the condensation reactions: (deoxy)ribose + uracil → nucleoside + water

	E (a.u.)	E_{rel} (kJ mol^{-1})	ΔH^o (kJ mol^{-1})	ΔG^o (kJ mol^{-1})	ΔS^o (J mol^{-1} K^{-1})
U1	−911.058673	15	33.4	22.5	36.7
U2	−911.064541	0	18.4	10.6	26.3
U3	−911.038707	68	11.1	19.1	−26.8
U4	−911.047459	45	−11.2	0.7	−39.9
U5	−911.022407	111	22.0	29.5	−25.2
U6	−911.024622	105	16.0	24.0	−26.9
D1	−835.839950	1	38.1	27.1	37.0
D2	−835.840374	0	36.5	23.1	45.1
D3	−835.819689	54	16.6	24.2	−25.6
D4	−835.821049	51	12.6	18.1	−18.4
D5	−835.804057	95	25.7	33.6	−26.5
D6	−835.805970	90	23.1	29.1	−20.0

residue and the uracil ring—a view supported by the ΔH^o value of D4, which is positive because of the absence of H-bonds of the type $^{furanose}H\cdots O=^{uracil}$, which stabilises the compound. For the same reason, the relative energy of isomer U4 is the lowest among all the hydroxy uridine tautomers. Only the condensation reactions to nucleosides that contain the oxo uracil tautomer have positive changes in entropy under standard conditions and in the gas phase.

Vertical excitation energies

Table 2 lists the vertical electronic excitation energies calculated for all the isomers and for a single uracil molecule, as well as the calculated vertical excitation energies of uracil tautomers (Scheme 1) optimized at the same theoretical level.

The calculated vertical excitation energies of the bright $^1\pi\pi^*$ state of the nucleosides that contain the uracil tautomer Ur1 (the most stable one) are in the interval 5.041–5.083 eV. This is in excellent agreement with the experimentally observed absorption maximum of uracil in the gas phase, 5.08 eV [19]. In the single uracil molecule (Ur1), we calculated 5.181 eV for the electron transition $^1\pi\rightarrow\pi^*$. Since the molecule of the tautomer Ur1 is planar, the excited states and the molecular orbitals of the compound can be assigned in symmetry—(A',A") and (a', a"), respectively. The calculated vertical excitation energies show that the TD B3LYP method can reproduce accurately the experimental positions of the maxima of the UV bands of organic compounds. It can be seen that rotation of Ur1 in directions U1→U2 and D1→D2 leads to a slight reduction of the vertical excitation energies of the $^1\pi\pi^*$ state, while the dark $^1n_O\pi^*$ states shift up. Some of the orbitals of U1 and Ur1 that are responsible for the excited states discussed here are illustrated in Fig. 2.

The fourth excited state ($^1n_O\pi^*$) of the nucleosides U1, U2 and D1 is a charge transfer state—from a (deoxy)ribose residue to uracil. Similar states are calculated also for U3, U4 and D3. Charge transfer states—from uracil to furanose moieties—are calculated for nucleosides D2, U5 and D5. Such states contribute to the considerable electroconductivity registered for the macromolecules DNA and RNA [20, 21].

The order of the $^1n_O\pi^*$ and $^1\pi\pi^*$ states is changed in nucleosides that contain the nonquinonic hydroxo uracil tautomer (Ur2). In these cases, the first excited state is the bright $^1\pi\pi^*$ state. The same positions of the excited electronic levels were calculated for the tautomer Ur2. These compounds have one $^1n_N\pi^*$ state, which is generated by electron transition from the lone-pair electrons of the sp^2 nitrogen atom to a π^* molecular orbital.

The first two low-lying excited states of the nucleosides with a semiquinonic hydroxo uracil tautomer (U5, U6, D5, and D6) are the dark $^1n_O\pi^*$ states. These are rather high, which means that the maxima of the UV absorption bands of these compounds should be observed in the higher energy region. In other words, such semiquinonic nucleosides would make only a minor contribution to the electroconductivity of nucleic acids.

Several decades ago, Miles et al. [22] found the peak maximum of the UV absorption spectrum of uridine in solution (pH=7) at 4.77 eV. We believe that this spectrum corresponds to the isomer U4, whose maximum should be at 4.721 eV (see Table 2). The calculated value is very close to the experimental value. The solvation effect is clear: the solvent increases the energy for the transition $\pi\rightarrow\pi^*$ in uridine by about 0.05 eV or 3 nm. In other words, a blue shift is observed when gas phase uridine is dissolved.

Conformational transformations of oxo (deoxy)uridine

The ground state conformational curves of the transformations U1↔U2 and D1↔D2 are illustrated in Fig. 3.

Table 2 Vertical excitation energies (E, eV) and oscillator strengths (f) of the four lowest singlet excited electronic states of isomers of uridine and deoxyuridine

	State	E	f×10^4		State	E	f×10^4
U1	$^1n_O\pi^*$	4.687	2	D1	$^1n_O\pi^*$	4.679	4
	$^1\pi\pi^*$	5.083	40		$^1\pi\pi^*$	5.071	2,006
	$^1n_O\pi^*$	5.415	14		$^1n_O\pi^*$	5.471	36
	$^1n_O\pi^*$ [a]	5.743	14		$^1n_O\pi^*$ [a]	5.740	5
U2	$^1n_O\pi^*$	4.747	5	D2	$^1n_O\pi^*$	4.702	6
	$^1\pi\pi^*$	5.051	2186		$^1\pi\pi^*$	5.041	2,147
	$^1n_O\pi^*$	5.550	3		$^1n_O\pi^*$	5.749	7
	$^1n_O\pi^*$ [a]	5.822	3		$^1\pi\sigma^*$ [b]	5.880	91
U3	$^1\pi\pi^*$	4.656	908	D3	$^1\pi\pi^*$	4.647	897
	$^1n_O\pi^*$ [a]	4.801	52		$^1n_O\pi^*$ [a]	4.792	23
	$^1n_O\pi^*$	5.251	145		$^1n_O\pi^*$	5.276	20
	$^1n_N\pi^*$	5.316	16		$^1n_N\pi^*$	5.356	29
U4	$^1\pi\pi^*$	4.721	1176	D4	$^1\pi\pi^*$	4.658	1,137
	$^1n_O\pi^*$	5.132	17		$^1n_O\pi^*$	4.922	7
	$^1n_O\pi^*$ [a]	5.297	65		$^1n_N\pi^*$	5.382	16
	$^1n_N\pi^*$	5.432	49		$^1n_O\pi^*$ [a]	5.672	307
U5	$^1n_O\pi^*$	4.345	0	D5	$^1n_O\pi^*$	4.324	0
	$^1n_O\pi^*$	4.971	4		$^1n_O\pi^*$	4.966	4
	$^1\pi\pi^*$	5.198	491		$^1\pi\pi^*$	5.183	522
	$^1\pi\sigma^*$ [b]	5.496	117		$^1\pi\sigma^*$ [b]	5.673	120
U6	$^1n_O\pi^*$	4.388	0	D6	$^1n_O\pi^*$	4.363	0
	$^1n_O\pi^*$	4.946	4		$^1n_O\pi^*$	4.969	4
	$^1\pi\pi^*$	5.112	530		$^1\pi\pi^*$	5.106	576
	$^1\pi\pi^*$	5.481	256		$^1\pi\pi^*$	5.519	838
Ur1	$^1n_O\pi^*$ (A")	4.669	0	Ur3	$^1\pi\pi^*$	4.643	587
	$^1\pi\pi^*$ (A')	5.181	1323		$^1n_O\pi^*$	4.819	4
	$^1\pi\sigma^*$ (A")	5.748	23		$^1n_N\pi^*$	5.295	15
	$^1n_O\pi^*$ (A")	5.780	0		$^1\pi\sigma^*$	5.602	24
Ur2	$^1n_O\pi^*$	4.335	0				
	$^1n_O\pi^*$	5.048	4				
	$^1\pi\pi^*$	5.256	489				
	$^1\pi\sigma^*$	5.495	10				

[a] Charge transfer state from ribose/deoxyribose to uracil

[b] Charge transfer state from uracil to ribose/deoxyribose

Figure 3 also shows the evolution of the excited states along the reaction coordinates $<C_{20}N_{10}C_2O_1$ for uridine and $<C_{19}N_{10}C_2O_1$ for deoxyuridine. It can be seen that the thermally induced [on the S_o potential energy surface (PES)] conformation, U1→U2 passes through a very high energy barrier of 1.630 eV (157 kJ mol^{-1}). Energetically much more favourable is the photochemical conformation passing through the bright $^1\pi\pi^*$ states of U1 and U2 and the dark charge transfer (CT) state $^1n\pi^*$. This transition is mediated by the two conical intersections $^1\pi\pi^*/^1n\pi^*$ and an insignificant energy barrier. The CT state $^1n\pi^*$ is over the transition state region on the ground state curve and is generated through a charge transfer from sugar to uracil. In general, the $^1n\pi^*$ and $^1\pi\pi^*$ curves follow the ground state curve with almost the same energy gradients.

The ground state conformational transformation D1→D2 is more favourable than that for uridine. The energy barrier is 1.287 eV (124 kJ mol^{-1}). However, the photochemical transformation is hindered considerably by high energy barriers. It can pass through the $^1\pi\pi^*$ states of D1 and D2 and the dark CT transfer state $^1\sigma\pi^*$. Conical intersections of the type $^1\pi\pi^*/^1\sigma\pi^*$ mediate this transition. Analysis of the energy curves shows that, in this case, the $^1n\pi^*$ and $^1\pi\pi^*$ curves follow the ground state curve as for uridine.

The results show that breaking the hydrogen bond $H_{15}\cdots O_{25}$ in uridine favours the photochemical conformation (as compared to deoxyuridine). The reason for this is that breaking this bond stabilises the dark CT state $^1n\pi^*$. The lack of such H-bonding during the conformation transition D1→D2 is responsible for the space hindrances at the small values of the reaction coordinates (at the beginning of the reaction after the minimum of D1). This also affects the shape of the reaction curves of the ground and excited states (see Fig. 3b).

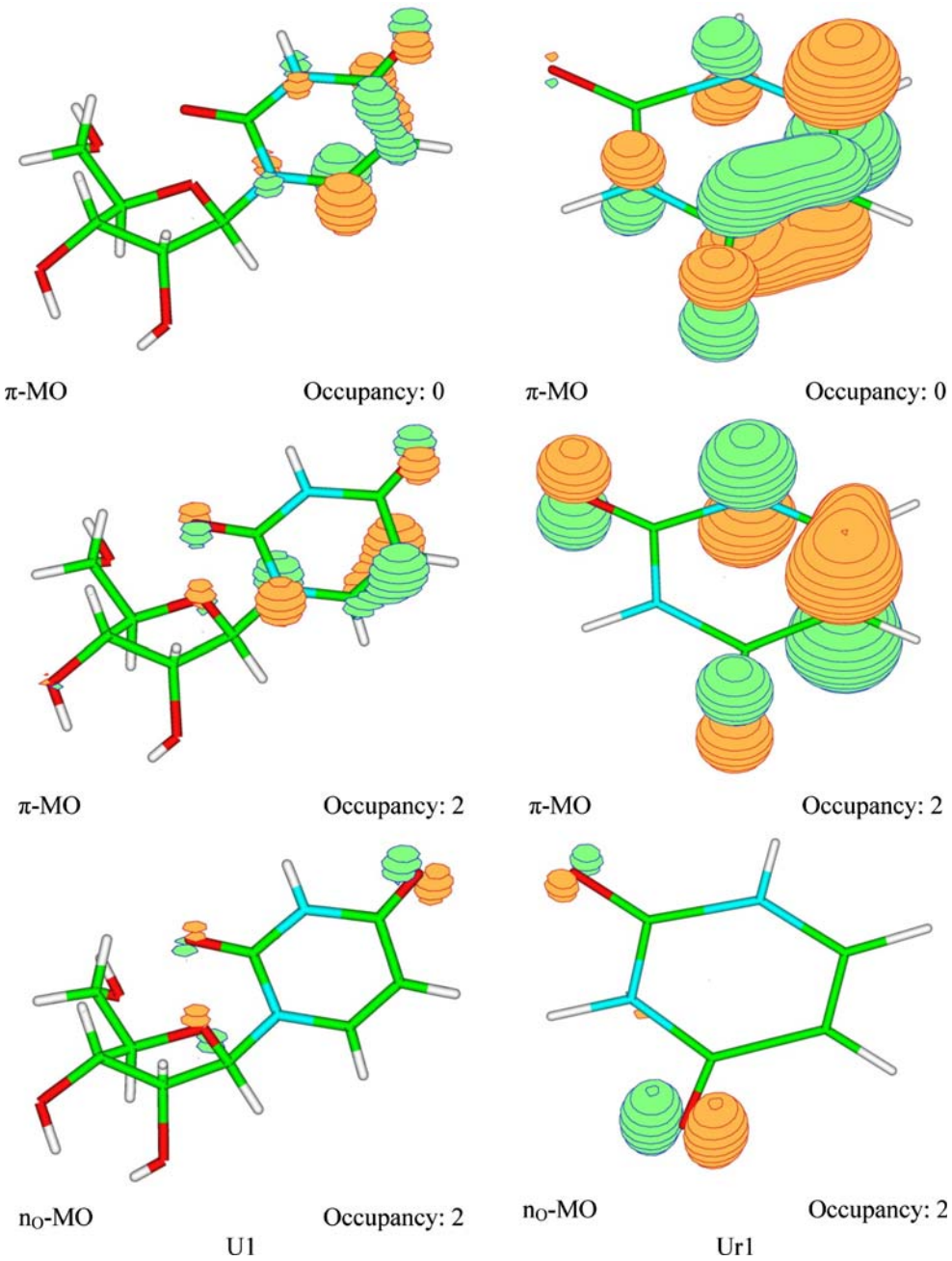

Fig. 2 Optimised molecular orbitals of U1 and Ur1 involved in electron transitions

Intramolecular proton transfers

The energy barriers of intramolecular proton transfers in uridine and deoxyuridine and the thermodynamic functions of these reactions are listed in Table 3.

The values in Table 3 show that the energy barriers of these intramolecular proton transfers are very high. Because of the nature of these processes (the proton is a small particle), one can expect tunnelling to occur. It can also be seen that the energy barriers of the reverse transformations are lower than those of the forward reactions. In other words, all structures of the transition states are closer to the products than to the reactants. Therefore, according to the Leffler-Hammond postulate [23, 24], the transition states can be assigned as product-like or "late". Comparing the energy barriers of the uridine and deoxyuridine reactions, one can conclude that the sugar residue does not contribute significantly to the kinetics of these reactions.

The calculated imaginary frequency in the vibration spectrum (parallel vibration mode) of each transition state is over $-1{,}900$ cm^{-1}, which clearly shows that the energy curves of the proton transitions are rather steep, and that the reactants and products lie in deep minima.

As a consequence of the Leffler-Hammond postulate, the proton transfers are endothermic (enthalpically disfavoured) and thermodynamically disfavoured (see Table 3). This

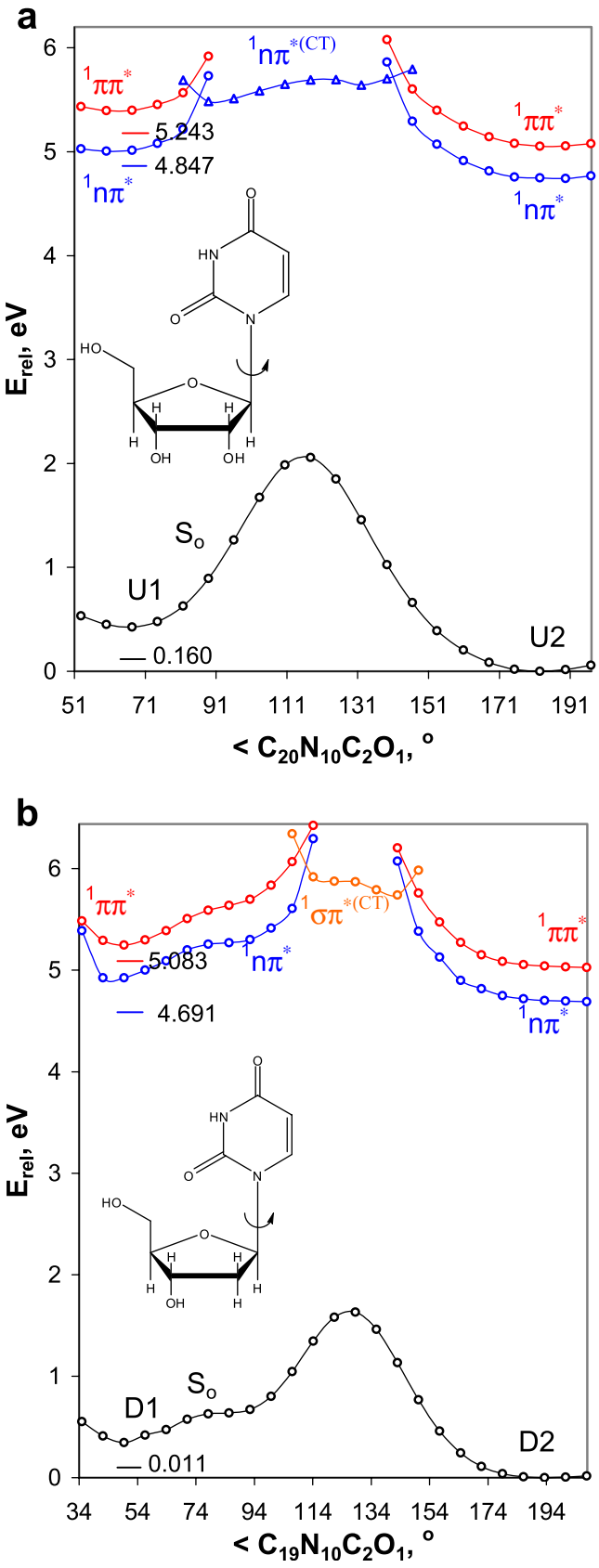

◀ **Fig. 3** Conformational potential energy surface (PES) of the ground and excited states of oxo (**a**) uridine and (**b**) deoxyuridine. The *coloured lines* designate the vertical excitation energies of the states of U1 and D1 as listed in Table 2

means that, in the gas phase, all equilibria are shifted towards the reactants. It can also be seen that the proton transfers are accompanied by insignificant entropy (steric) changes, which probably means that only a limited number of internal coordinates are changed during the proton transfers, most likely those connected with the moving proton.

Conclusions

The calculations performed (at the DFT and TD DFT level) on the stability, excited states and intramolecular proton transfers in uridine and deoxyuridine led to the following major conclusions: (1) the formation of H-bonds between uracil and the ribose ring stabilises the H-bonds formed between the two OH groups of the ribose ring; (2) nucleosides that contain the oxo form of uridine are dominant; (3) TD DFT calculations reproduce vertical excitation energies accurately, yielding values close to reported experimental data [19, 22]; (4) the excited state analysis proved the reported UV absorption maximum of uridine in solution at 4.77 eV [22] corresponds to uridine involving the hydroxo uracil tautomer; (5) it was established that the first and second excited states of oxo uracil nucleosides are $^1n\pi^*$ and $^1\pi\pi^*$, respectively, like these of uracil; (6) the rotation of the oxo uracil ring in uridine is much more likely to occur in the excited state than in the ground state. In deoxyuridine, rotation in the excited state is hindered by relatively high energy barriers; and (7) high

Table 3 Energy barriers and thermodynamic functions of the intramolecular proton transfer reactions in uridine and deoxyuridine (kJ mol^{-1})

	Energy barriers				ΔH^o_{298}	ΔG^o_{298}	$T\Delta S^o_{298}$
	$E_{forward}$	$E_{reverse}$	$E^o_{forward}$	$E^o_{reverse}$			
U1⇄U3	191	139	177	126	50.0	51.7	−1.7
U1⇄U5	216	121	201	108	93.4	92.7	0.7
U2⇄U4	187	141	173	128	43.7	45.1	−1.4
U2⇄U6	223	118	207	106	102.4	99.0	3.4
D1⇄D3	192	139	177	125	51.7	52.2	−0.5
D1⇄D5	213	119	198	106	92.4	92.1	0.3
D2⇄D4	190	139	176	126	49.4	50.1	−0.7
D2⇄D6	217	124	202	111	91.5	91.7	−0.2

$E^o_{forward/reverse}$ - energy difference between the zero-point levels of the transition state and the reactant/product

energy barriers between intramolecular proton transfers in the ground state were found.

References

1. Hosein S (2004) Canadian AIDS Treatment Information Exchange (http://www.thebody.com/content/art30244.html, accessed: 14.07.2009)
2. Walker UA, Langmann P, Miehle N, Zilly M, Klinker H, Petschner F (2004) AIDS 187:1085–1086
3. Dagan T, Sable C, Bray J, Gerschenson M (2002) Mitochondrion 1:397–412
4. Carlezon WA Jr, Mague SD, Parow AM, Stoll AL, Cohen BM, Renshaw PF (2005) Biol Psychiatry 57:343–350
5. Nicholas RA, Watt WC, Lazarowski ER, Li Q, Harden K (1996) Mol Pharmacol 50:224–229
6. Qu W, Tabisz GC (2006) J Chem Phys 124:184305–184314
7. Bureekaew S, Hasegawa J, Nakatsuji H (2006) Chem Phys Lett 425:367–371
8. Merchan M, Gonzalez-Luque R, Climent T, Serrano-Andres L, Rodriguez E, Reguero M, Pelaez D (2006) J Phys Chem, B 110:26471–26476
9. Matsika S (2004) J Phys Chem A 108:7584–7590
10. Santoro F, Barone V, Gustavsson T, Improta R (2006) J Am Chem Soc 128:16312–16322
11. Lorentzon J, Fülscher MP, Ross BO (1995) J Am Chem Soc 117:9265–9273
12. Mezzache S, Alves S, Pepe C, Quelquejeu M, Fournier F, Valery JM, Tabet JC (2005) J Mass Spectrom 40:722–730
13. Green EA, Rosenstein RD, Shiono R, Abraham DJ (1975) Acta Cryst B 31:102–107
14. Rahman A, Wilson HR (1972) Acta Cryst B 28:2260–2270
15. Ivanov AY, Krasnokutski SA, Sheina G, Blagoi YP (2003) Spectrochim Acta A 59:1959–1973
16. Atkins PW (1986) Physical chemistry, 3rd edn. Oxford University Press, Oxford
17. Frisch MJ, Trucks GW, Schlegel HB, Scuseria GE, Robb MA, Cheeseman JR, Zakrzewski VG, Montgomery JA Jr, Stratmann RE, Burant JC, Dapprich S, Millam JM, Daniels AD, Kudin KN, Strain MC, Farkas O, Tomasi J, Barone V, Cossi M, Cammi R, Mennucci B, Pomelli C, Adamo C, Clifford S, Ochterski J, Petersson GA, Ayala PY, Cui Q, Morokuma K, Malick DK, Rabuck AD, Raghavachari K, Foresman JB, Cioslowski J, Ortiz JV, Baboul AG, Stefanov BB, Liu G, Liashenko A, Piskorz P, Komaromi I, Gomperts R, Martin RL, Fox DJ, Keith T, Al-Laham MA, Peng CY, Nanayakkara A, Gonzalez C, Challacombe M, Gill PMW, Johnson B, Chen W, Wong MW, Andres JL, Gonzalez C, Head-Gordon M, Replogle ES, Pople JA (1998) Gaussian 98, Rev A.7. Gaussian Inc, Pittsburgh PA
18. Zhurko GA, Zhurko DA (2007) ChemCraft, ver 1.5 (build 282). http://www.softpedia.com/
19. Clark LB, Peschel GG, Tinoco I Jr (1965) J Phys Chem 69:3615–3618
20. Okahata Y, Nakayama H (2000) In: Abstacts, 15th Symposium on Biofunctional Chemistry, pp 128–129
21. Nakayama H, Ohno H, Okahata Y (2001) Chem Commun (Camb) 21:2300–2301
22. Miles DW, Robins RK, Eyring H (1967) Proc Natl Acad Sci USA 57:1139–1145
23. Hammond GS (1955) J Am Chem Soc 77:334–338
24. Leffler JE (1953) Science 117:340–341